

See discussions, stats, and author profiles for this publication at: <https://www.researchgate.net/publication/51739956>

Difluoromethylbenzoxazole Pyrimidine Thioether Derivatives: A Novel Class of Potent Non-Nucleoside HIV-1 Reverse Transcriptase Inhibitors

ARTICLE *in* JOURNAL OF MEDICINAL CHEMISTRY · DECEMBER 2011

Impact Factor: 5.45 · DOI: 10.1021/jm200766b · Source: PubMed

CITATIONS

18

READS

67

6 AUTHORS, INCLUDING:



Maurice Medebielle

Claude Bernard University Lyon 1

134 PUBLICATIONS 1,938 CITATIONS

SEE PROFILE



Jérôme Guillemont

Johnson & Johnson

53 PUBLICATIONS 2,553 CITATIONS

SEE PROFILE



Johan Unge

Lund University

14 PUBLICATIONS 118 CITATIONS

SEE PROFILE



Dirk Jochmans

University of Leuven

33 PUBLICATIONS 1,081 CITATIONS

SEE PROFILE

Difluoromethylbenzoxazole Pyrimidine Thioether Derivatives: A Novel Class of Potent Non-Nucleoside HIV-1 Reverse Transcriptase Inhibitors[†]

Jérémie Boyer,[‡] Eric Arnoult,[§] Maurice Médebielle,^{*,‡} Jérôme Guillemont,^{*,§} Johan Unge,^{*,||} and Dirk Jochmans^{⊥,‡}

[‡]Université de Lyon, Université Claude Bernard Lyon 1, Institut de Chimie et Biochimie Moléculaires et Supramoléculaires (ICBMS), UMR CNRS-UCBL-INSA, Equipe "Synthèse de Molécules d'Intérêt Thérapeutique (SMITH)", Bâtiment Curien, 43 Boulevard du 11 Novembre 1918, F-69622 Villeurbanne, France

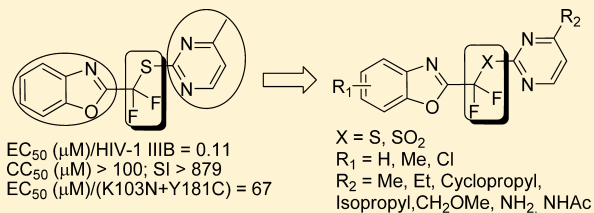
[§]Chemistry Lead Antimicrobial Research, Janssen-Cilag/Tibotec, Campus de Maigremont BP615, F-27106 Val de Reuil Cedex, France

^{||}MAX-lab, Lund University, P.O. Box 118, SE-221 00 Lund, Sweden

[⊥]Tibotec-Virco BVBA, A Division of Janssen Pharmaceutical Companies of Johnson & Johnson, Turnhoutseweg 30, BE-2340 Beerse, Belgium

Supporting Information

ABSTRACT: This paper reports the synthesis and antiviral properties of new difluoromethylbenzoxazole (DFMB) pyrimidine thioether derivatives as non-nucleoside HIV-1 reverse transcriptase inhibitors. By use of a combination of structural biology study and traditional medicinal chemistry, several members of this novel class were synthesized using a single electron transfer chain process (radical nucleophilic substitution, $S_{RN}1$) and were found to be potent against wild-type HIV-1 reverse transcriptase, with low cytotoxicity but with moderate activity against drug-resistant strains. The most promising compound **24** showed a significant EC_{50} value close to 6.4 nM against HIV-1 IIB, a moderate EC_{50} value close to 54 μ M against an NNRTI resistant double mutant (K103N + Y181C), but an excellent selectivity index >15477 ($CC_{50} > 100$ μ M).



INTRODUCTION

Non-nucleoside reverse transcriptase inhibitors (NNRTIs) have been shown to be a key component of highly active antiretroviral therapy (HAART). The use of NNRTIs has become part of standard combination antiviral therapies producing very effective drugs with clinical efficacy comparable to that of other antiviral regimens. There is, however, a critical issue with the emergence of drug-resistant HIV-1 mutants, and a need has arisen for novel NNRTIs with improved activity profiles. There are currently three commercially available first generation NNRTIs: efavirenz, nevirapine, and delavirdine (Figure 1).¹

Recently, the second generation NNRTI etravirine (TMC-125, Figure 1), a diarylpyrimidine (DAPY) derivative, has been approved by the FDA and has demonstrated activity toward a number of clinically observed mutations.² Further research to develop an even better DAPY derivative has led to the discovery of an advanced NNRTI, rilpivirine (TMC-278, Figure 1), which has been approved by the FDA in February 2011 and showed better potency and pharmacological profiles than etravirine.²

Quite close analogues of the DAPY family, such as diarylpyridine **1**,³ diarylanilines **2** and **3**,³ and pyrrolopyrimi-

dines **4** (RDEA-640) and **5** (RDEA-427, preclinical),⁴ have been recently disclosed and displayed similar or better potency than etravirine (Figure SI-1 of Supporting Information). Additional structures have been disclosed from major pharmaceutical companies, and some of them are already in clinical trials such as trisubstituted thioacetanilide triazole **6** (RDEA-806, phase II),⁴ arylphosphoindole derivative **7** (IDX-899/GSK-2248761, phase II),⁵ diaryl ether/pyrazolo[3,4-*b*]pyridine **8** (MK-4965, phase I) (Figure SI-1 of Supporting Information).⁶ Compound **9** (L-696,229)⁷ and some analogues (**10** and **11**) are potent NNRTIs (Figure SI-2 of Supporting Information) and were discovered in a screening program at Merck. Although their clinical development was suspended because of the emergence of resistance, the pyridine-2(1H)-ones remained an attractive pharmacophore and various synthetic programs were initiated in order to discover new molecules that could circumvent the resistance of the Merck pyridinones.^{8,9} Despite that a number of molecules have been shown to be very potent at nanomolar concentrations against clinically relevant mutant strains, none of them have been pushed forward to clinical trials.

Received: June 14, 2011

Published: October 21, 2011



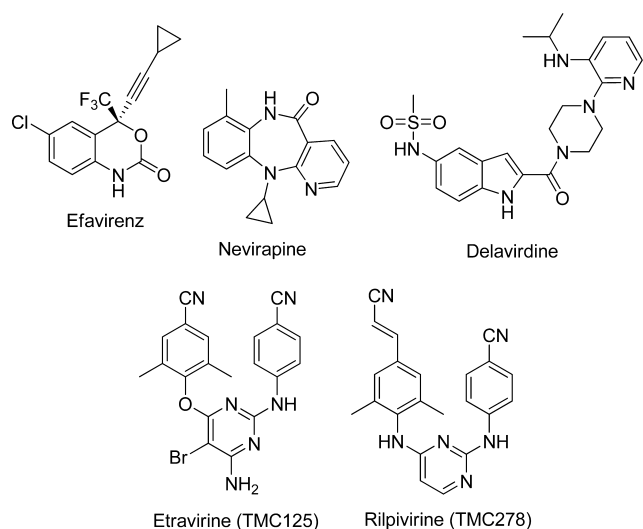


Figure 1. Currently marketed NNRTIs and the most advanced NNRTI TMC-278.

Some years ago, a research program directed to the development of efficient and mild approaches to prepare difluoromethylene substituted aromatics and heterocycles of biological interest was launched. As part of these investigations, we envisaged selectively incorporating fluorine substituents into structural analogues of **9** in order to determine the impact of such substitution on biological activity.^{10–12} Dramatic enhancements of activity have been reported in many cases for partially fluorinated analogues of biologically active compounds;¹³ fluorinated substituted aromatics and heterocycles have found broad applications in agrochemicals and anticancer and antiviral agents. The similarity in size makes the fluorine an obvious candidate to replace hydrogen, often without significant disturbance of the molecular geometry and shape. In addition it is now recognized that fluorine substitution can reduce or block metabolic pathways selectively, affect substantially the pK_a of a molecule to modify the binding and the pharmacokinetic properties of pharmaceutical agents and change also the lipophilicity of a drug candidate, to cite a few.^{14–16} In 1998 the first series of simpler analogues of **9** where the $-\text{CH}_2\text{CH}_2-$ spacer was replaced with a $-\text{CF}_2\text{CHOH}-$ ¹⁰ were prepared using a novel methodology based on the tetrakis(dimethylamino)ethylene (TDAE)¹⁷

reductive cleavage of 2-(bromodifluoromethyl)benzoxazole and bromodifluoromethyloxadiazole derivatives with subsequent coupling reactions of the corresponding stable difluoromethyl anions with commercially available heteroaldehyde and ketones. Unfortunately the corresponding carbinols thus obtained were devoid of any activity when tested against HIV-1 virus ($\text{IC}_{50} > 50 \mu\text{M}$; Figure 2). At that time, it was postulated that the hydroxyl group may block efficient binding to the enzyme; therefore, in a subsequent work the hydroxyl of such carbinols was transformed into other functionalities via straightforward synthetic sequences.¹² However these new molecules bearing $-\text{CF}_2\text{CH}(\text{OR})-$ ($\text{R} = \text{Me}, \text{COCH}_3, \text{COAr}$), $-\text{CF}_2\text{CHF}-$, $-\text{CF}_2\text{CO}-$, $-\text{CF}_2\text{CF}_2-$, and $-\text{CF}_2\text{CH}_2-$ linkers were again devoid of significant activity ($\text{IC}_{50} > 50 \mu\text{M}$; Figure 2).¹² However, with a heteroatom ($\text{Y} = \text{S}, \text{O}$) replacing one of the $-\text{CH}_2$, a number of molecules that were obtained using the $\text{S}_{\text{RN}}1$ ¹⁸ coupling methodology of 2-(bromodifluoromethyl)-benzoxazole with commercially available heterocyclic thiols and phenolic compounds were found to be moderately to quite active (Figure 3).¹² In this last series, the two most active compounds **12** and **13** tested at the NIH were found to be quite potent with **12** being the most active ($\text{EC}_{50} = 64.6 \text{ nM}$) against HIV-1 IIIB. It was also found that the pyrimidine thioether **14** was 10 times more active than its nonfluorinated analogue **15** (Figure 3). Although **12** was quite active, it was inactive against a number of mutant strains of HIV. Despite the fact that these molecules were only active against HIV-1 wild-type, a new class of potent anti-HIV-1 agents were thus obtained in only two steps using commercially available reagents (aldehydes, thiols, and phenols). However, there was still some unclear reasons why the carbinols and their chemically derived compounds were totally inactive compare to the thioethers and also to a lesser extent the ether derivatives. Worth mentioning was that at the time we started the project in 1997–1998, there were two relevant papers from Pharmacia & Upjohn Company^{19,20} including two patents^{21,22} describing promising results with pyrimidine thioether derivatives; however, for unknown reasons these series were not pursued.

In a collaborative project with Tibotec, it was then decided to re-evaluate the biological activity of **12** and **13**, to test them against clinically relevant double mutant strain (K103N + Y181C), and to improve the overall antiviral profile of the hit **12** using structural biology and medicinal chemistry. The

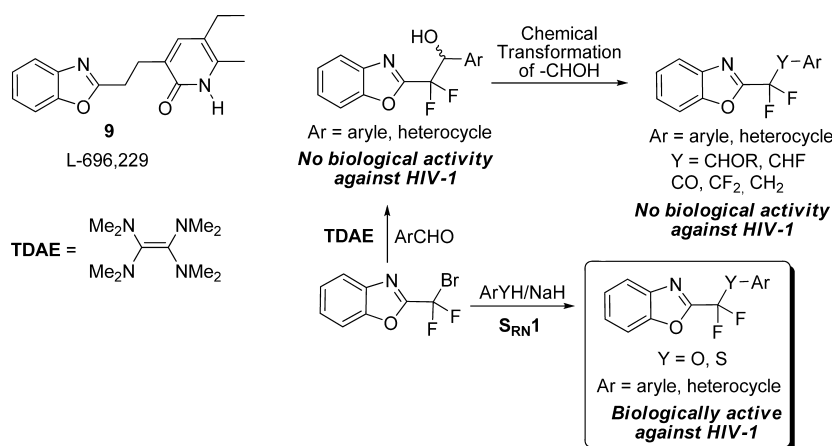


Figure 2. Benzoxazole derivatives with a CF_2 group.

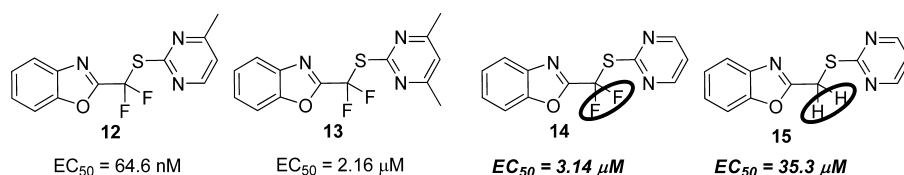


Figure 3. Biologically active benzoxazoles with a $-\text{CF}_2\text{S}-$ spacer.

medicinal chemistry effort concentrated on structural modifications on the western wing (benzoxazole) and eastern wing (pyrimidine), keeping the $-\text{CF}_2\text{S}-$ linker intact.

RESULTS

By use of standard antiviral assays, it was found that **12** and **13** were indeed potent HIV-1 inhibitors with similar activities as previously reported by NIH (Figure 4). Compound **12**, with an

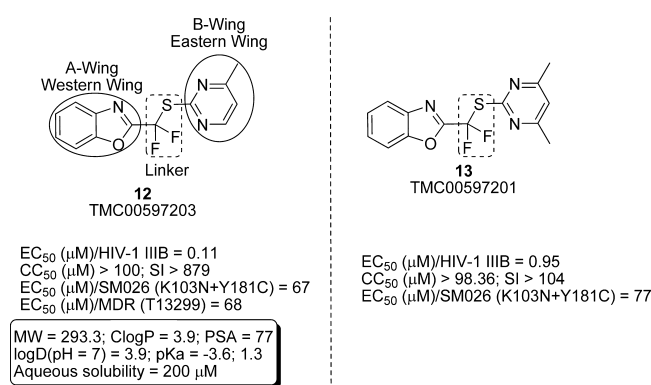


Figure 4. Biological data and physicochemical properties of the hit **12** and its analogue **13**.

EC_{50} equal to 111 nM against HIV-1 IIIB and with low cytotoxicity ($CC_{50} > 100 \text{ } \mu\text{M}$, SI > 879), remained the most active compound but with still a poor anti-HIV activity ($EC_{50} \approx 67 \text{ } \mu\text{M}$) against the double mutant (K103N + Y181C). Moreover, compound **12** displayed very good physicochemical properties (Figure 4) but also an excellent permeability in the Caco-2 cell-based assay ($P_{\text{app}} = 34.6 \times 10^{-6} \text{ cm s}^{-1}$), a good stability in human liver microsomes (90% recovery after 15 min), and no issue for cytochrome P450 inhibition (<30% inhibition for CYP3A4, CYP2C9, CYP2D6). These encouraging data incited us to continue exploration of the aryl moieties.

Structural Biology. Cocystal structures could provide information that could help in the design of inhibitors. To support this process, two HIV-1 reverse transcriptase mutants, Phe227Cys and Phe227Leu, were cocrystallized with compound **12** and the structures were solved at a resolution of 2.75 and 2.1 Å, respectively, and with R/R_{free} of 26/33 and 25/29, respectively (see Table 1 in Supporting Information). F227C/E478Q and F227L/E7478Q double mutants were chosen, since better (big) crystals were usually produced, and in addition the E478Q mutation induces reduction of flexibility by local reduction of negative charges in the active site of RNAsH.

The key interactions of compound **12** with the non-nucleoside inhibitor binding pocket (NNIBP) of HIV-1 RT mutants Phe227Cys and Phe227Leu are shown in Figure 5. The distances between the compound and the mutated residue are 5.2 Å (Leu) and 5 Å (Cys). In both structures, it is obvious that the mutated residues Phe227Leu and Phe227Cys are too

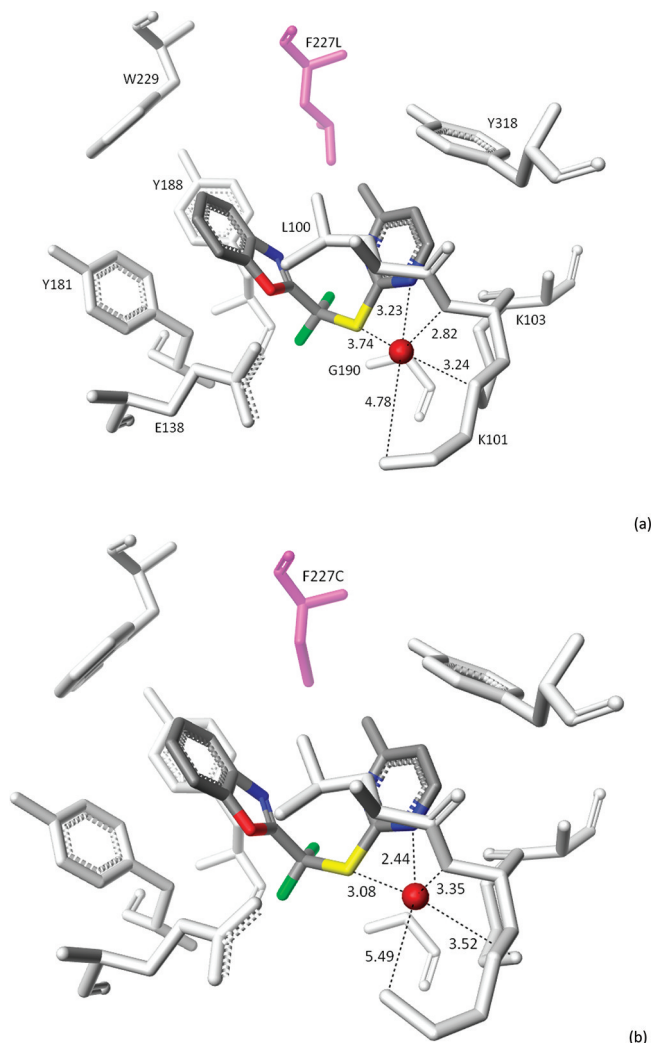


Figure 5. NNRTI binding pocket of (a) F227L (PDB access number 2ykn) and (b) F227C (PDB access number 2ykm) HIV reverse transcriptase bound with compound **12**. The inhibitor is shown in capped sticks. The mutated amino acids F227L and F227C are highlighted in magenta. The crystallized water molecule, located in this area, is shown as a red sphere. For clarity, only the first layer amino acids surrounding the inhibitor are shown (at a distance of 5 Å). The hydrogen atoms are not shown. The structures were created with Benchware 3D Explorer on a Windows workstation (Tripos Associates, St. Louis, MO, U.S.).

far from the ligand for any direct interaction. It is unlikely that the binding of the **12** is affected by any of these mutations.

The compound, which adopts a typical butterfly-like conformation frequently found in most of the NNRTIs,²³ was easily interpreted in the structures. The position of the benzoxazole group of compound **12** is stabilized by π -stacking interactions with aromatic side chains of Tyr181 at the shortest distance of 3.6 Å and of Tyr188 at a distance of 3.8 Å. The

continuous electron density between the benzoxazole and this Tyr188 side chain reinforces this assumption. We also found an edge–face π -systems interaction to the benzene ring of Trp229, with a closest distance of 3.8 Å between the closest atoms (Figure SI-3 of Supporting Information). The pyrimidine ring makes another edge–face interaction to Tyr318 in the eastern wing, 3.6 Å apart.

These ring interactions are further stabilized by the snug fit into the binding groove of the protein. Concerning the linker, the fluorine atoms rest on the interface of two NNIBP β strands. The sulfur atom is situated in a well-formed hydrophobic pocket, constituted by the hydrophobic parts of residues Leu100, Val179, Gly190, and Lys103 at typical van Der Waals distances. The shape of the fluorine and the sulfur pockets determine the orientation of the compound, and larger structures in the linker region would not fit into these hydrophobic pockets. In the case of other NNRTIs, rilpivirine, for instance,²⁴ whose linker region contains a ring structure, the ligand is rotated, leaving the linker region outside these pockets in order to accommodate the extra atoms (Figure 6).

The role of the fluorine atom for the enhanced activity compared to hydrogen atoms in the linker merits some comments. Fluorine is known to have a larger van der Waals radius, and it may be speculated that the fluorine atoms prevent the ligand from moving too deep into the pocket, thereby maintaining a better position for the π -stacking bonds of the benzoxazole group. One can also think that the fluorine atom may interact favorably with backbone and side chain amide groups in the enzyme pocket as previously observed in some other studies;¹⁶ however, it is not obvious from our crystallographic data that such interactions do occur really with **12**. In addition to the fluorine effect, a critical key to observe any inhibitory activity is the presence of a sulfur atom, since the molecules having a $-\text{CF}_2-$ adjacent to a carbon are totally inactive. A cocrystallized water molecule was found in both structures, at the same place, between one of the nitrogen of the pyrimidine and the sulfur atom (compound **12**), the backbone of Lys101, and the side chain of Lys101/103, offering to this water molecule plenty of H-bonds network. A comparison of rilpivirine²⁵ and **12** cocrystal structures (Figure 6) shows a pretty good superimposition of this water molecule and the nitrogen of the pyrimidine in rilpivirine, showing the same H-bonds interactions. The H-bonds network is believed to be an important additional contributing factor for RT inhibitors binding affinity.

Medicinal Chemistry. On the basis of structural biology data, a first series of compounds **17–28** were designed (Figure 7). These new molecules modified on either the benzoxazole or pyrimidine rings were developed with the aim to improve in the first instance the activity against the wild type and then on the double mutant. Basically we wanted to explore the impact on the antiviral activity when replacing the methyl moiety on the pyrimidine ring of **12** with larger substitutions such as cyclopropyl, ethyl, and isopropyl and see if sterically more demanding substitutions will be tolerated. Structural modifications (methyl, chlorine) on the benzoxazole ring were also envisaged to determine if such moieties will induce better π -stacking with both Tyr188 and Tyr181, as well as more favorable interactions with Tyr318 and Trp229. From the cocrystallized structures of **12**, there appear to be enough space to introduce such modifications that maybe well tolerated. On the pyrimidine ring additional substitutions (NH_2 , OH, CH_2OMe) were also thought in order to find out if they will

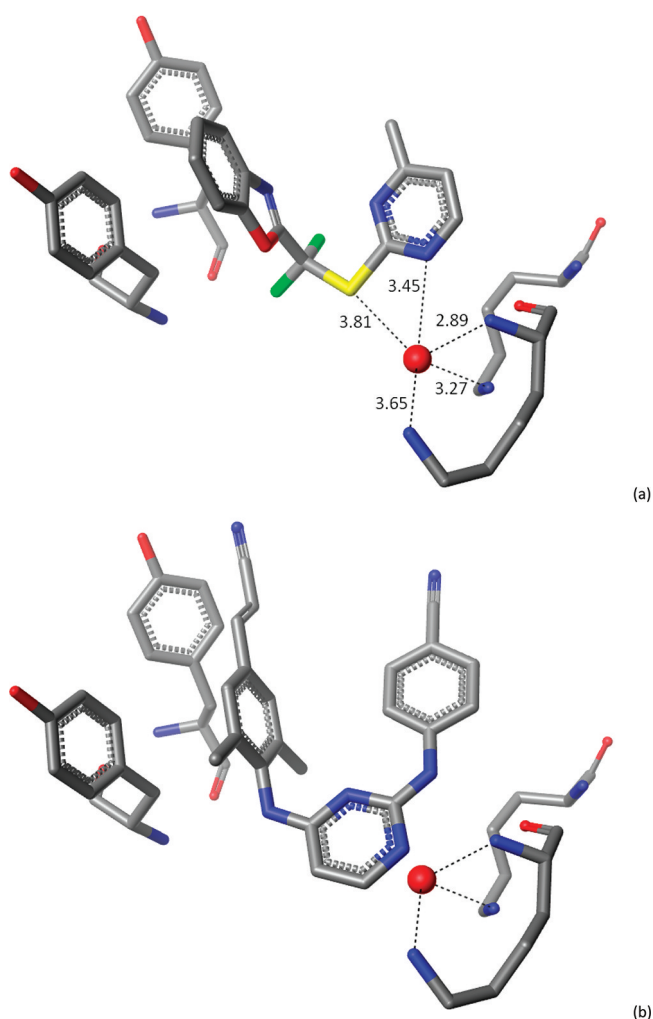


Figure 6. Comparison of binding mode of (a) compound **12** and (b) TMC278 (PDB accession number 3MEE). (b) The TMC278 X-ray structure was superimposed onto the NNRTI binding site of compound **12**. The water molecule that crystallizes in the presence of compound **12** is in close contact with the aminopyrimidine of TMC278, probably displaced by the nitrogen atom in the TMC278-RT binding site.

create more proper hydrogen bonds with key amino acids Lys101 and Lys103 that are missing to some extent with hit **12**. Such typical variations have been already well studied with other NNRTIs and particularly TMC278 and have been proven to be beneficial for improving the activity against wild type and mutants. In addition introducing flexibility in the binding mode of the NNRTI to accommodate the “wobble and jiggle” hypothesis will be desirable, however, these latter modifications are far more difficult to introduce by design and perhaps only feasible by a trial and error approach.²⁵

All the compounds are obtained from the coupling of a suitable thiopyrimidine anion (generated in situ with sodium hydride in anhydrous *N,N*-dimethylformamide) in the presence of the corresponding 2-(bromodifluoromethyl)benzoxazole, following the $\text{S}_{\text{RN}}1$ mechanism.¹¹ The starting 2-(bromodifluoromethyl)benzoxazoles **29–33** are prepared from the cyclization of the corresponding amides **34–37** in the presence of polyphosphoric acid under heating following our published procedure (Scheme 1).²⁶

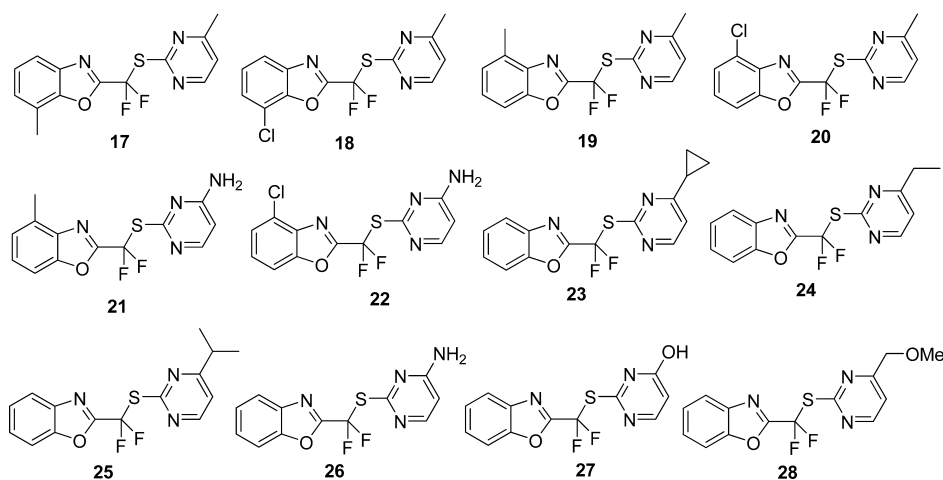
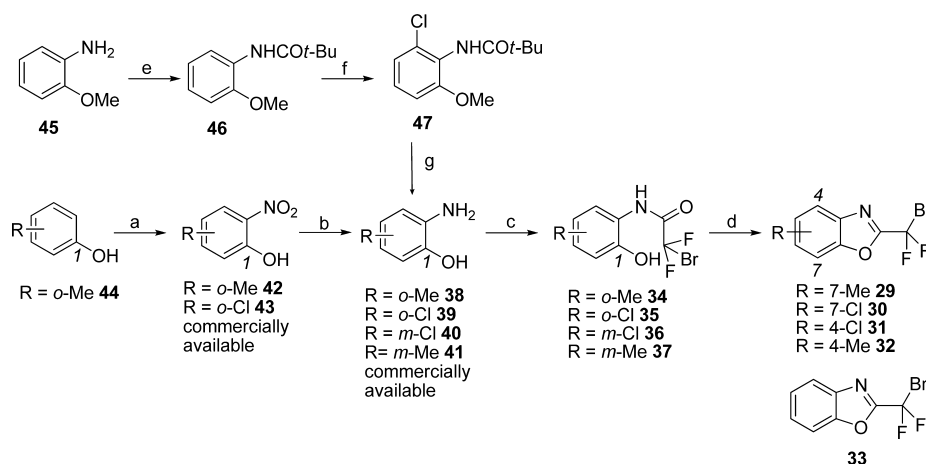
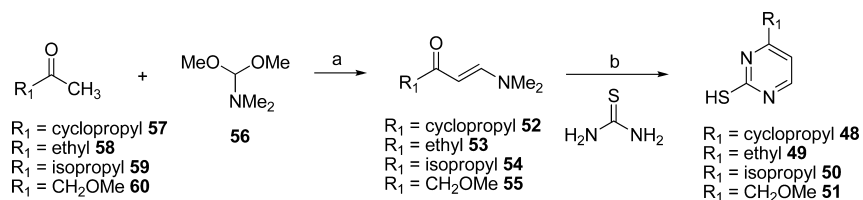


Figure 7. New designed compounds based on structural biology.

Scheme 1^a

^a(a) Claycop = $\text{Cu}(\text{NO}_3)_2$ + montmorillonite K10 clay for **42**, 48%. (b) $\text{Zn} + \text{AcOH}/\text{MeOH}$: **38**, 64%; **39**, 81%. (c) $\text{BrCF}_2\text{CO}_2\text{Et} + \text{Et}_3\text{N}/\text{EtOAc}$ under reflux: **34**, 76%; **35**, 72%; **36**, 22%; **37**, 78%. (d) PPA at 150°C , then aqueous NH_3 : **29**, 45%; **30**, 43%; **31**, 37%; **32**, 80%. (e) Pivaloyl chloride + $\text{Et}_3\text{N}/\text{CH}_2\text{Cl}_2$: **46**, >95%. (f) $n\text{-BuLi}$ (2.4 equiv) + $\text{C}_2\text{Cl}_6/\text{THF}$: **47**, 72%. (g) HBr at 120°C for **40**, 92%.

Scheme 2^a

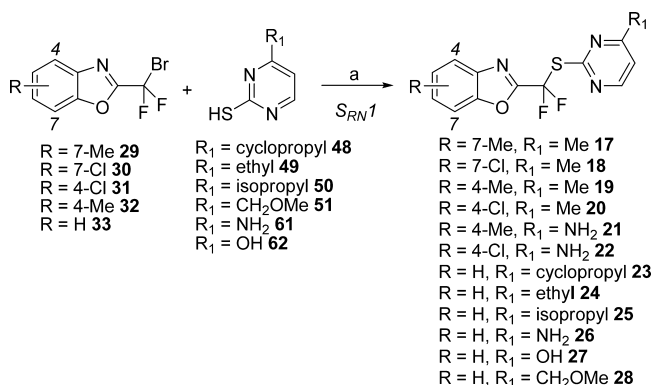
^a(a) Neat, reflux or neat, 110°C (sealed tube): **52**, 66%; **53**, 39%; **54**, 50%; **55**, 45%. (b) MeONa/EtOH , 24 h: **48**, 47%; **49**, 10%; **50**, 38%; **51**, 38%.

The amides **34–37** are prepared from key amino phenols **38–41** (**41** is commercially available) that are obtained (a) in one step for **39** from the zinc reduction in acetic acid and MeOH of commercially available **43**, (b) in two steps for **38** through nitration of **44** using copper(II) nitrate supported on Montmorillonite clay K10²⁷ and further reduction of **42** with zinc in acetic acid and MeOH , and (c) in three steps for **40** from known **46**²⁸ using an ortho-lithiation strategy and final one-pot deprotection of the methoxy group and carbamate of **47** in HBr at 120°C . Compound **47** is known from a patent,²⁹ but we have improved its yield (72% vs 41% in the patent)

using 2.4 equiv of $n\text{-BuLi}$ in THF without TMEDA (instead of 1 equiv of $n\text{-BuLi}$ in Et_2O in the presence of TMEDA). The amides thus obtained by reaction with ethyl bromodifluoroacetate in refluxing ethyl acetate in the presence of triethylamine, are further cyclized into the corresponding benzoxazoles using polyphosphoric acid (PPA) at 150°C with careful workup with aqueous NH_3 , which prevents the conversion of the benzoxazoles back to the amides, by acid-catalyzed hydrolysis. The benzoxazoles are usually isolated by silica gel chromatography or can be distilled (larger scale).

Thiopyrimidines **48**,³⁰ **49**,³¹ **50**, and **51** are prepared from the condensation of thiourea and suitable enamino ketones **52**,³² **53**,³³ **54**,³⁴ and **55**³⁵ that can be prepared from *N,N*-dimethylformamidedimethyl acetal **56** and appropriate commercially available ketones **57–60** (Scheme 2). Most of the enaminoketones were obtained in moderate yields after silica gel chromatography, since the conversion of the starting ketones is not complete, with also the formation of regioisomeric enaminoketones. Classical thiopyrimidine ring formation was done using thiourea under basic conditions using MeONa as the base (excess) in refluxing absolute ethanol as solvent. The final products were usually obtained after silica gel chromatography (to remove unreacted thiourea) and purification of the resulting solid from precipitation with MeOH or CH₂Cl₂/pentane mixture (to remove unreacted enaminoketone). Surprisingly the thiopyrimidine **49** was only obtained in a 10% isolated yield. 4-Amino-2-thiopyrimidine **61** that is required to prepare targets **21**, **22**, and **26** is commercially available as well as 2-thiouracil **62** to prepare target **27**.

With all the reactants in hand, the S_{RN1} reactions of **29–33** with the appropriate thiopyrimidines **48–51** and **61–62** were run in anhydrous DMF at 60–100 °C. The reactions were usually monitored by TLC and ¹⁹F NMR until almost complete conversion of the starting 2-(bromodifluoromethyl)benzoxazole (Scheme 3). Despite many attempts, the coupling product **27**

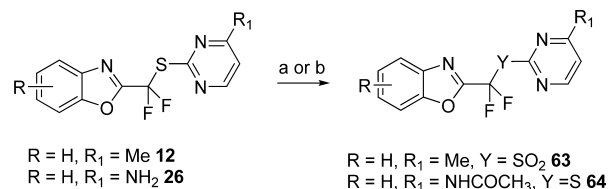
Scheme 3^a

^a(a) NaH (2.5–3.5 equiv), DMF, 60–100 °C, 15–18 h: **17**, 43%; **18**, 56%; **19**, 80%; **20**, 47%; **21**, 24%; **22**, 54%; **23**, 75%; **24**, 10%; **25**, 35%; **26**, 80%; **27**, 0%; **28**, 50%.

from the reaction of **33** with 2-thiouracil **62** was unsuccessful even at temperature close to 100 °C. Surprisingly the S_{RN1} reaction product **24** was only obtained in 10%, since the starting thiol **49** was contaminated with some thiourea and therefore required careful purification.

Two additional compounds **63** and **64** were also synthesized from hit **12** and coupling product **26** (Scheme 4). The sulfone **63** was obtained in a moderate 46% yield after silica gel chromatography from the *m*CPBA oxidation (8 equiv) of sulfanyl compound **12** in dichloromethane, since a mixture of sulfoxide and unidentified fluorinated impurities was always obtained. Amide compound **64** was obtained in a nonoptimized 35% yield from the acetic anhydride reaction in pyridine in the presence of a catalytic amount of *N,N*-dimethylaminopyridine from coupling product **26**.

Antiviral Activity. All the compounds thus synthesized were evaluated against HIV-1 IIIB and the double mutant (K103N + Y181C) NNRTI resistant strains (Table 2).

Scheme 4^a

^a(a) *m*CPBA (8 equiv), CH₂Cl₂, 0 °C to room temp, 15 h: **63**, 46%.
(b) Ac₂O, pyridine, DMAP cat., 55 °C, 7 h: **64**, 35%.

Table 2. Data of Compounds **12**, **13**, **17–28**, **63**, and **64**

compd	IIIB EC ₅₀ (μM) ^a	CC ₅₀ (μM) ^b	SI ^c	K103N + Y181C EC ₅₀ (μM)
12	0.11	>100.0	>800	67.0
13	0.95	>98.4	>100	77.2
17	0.20	>98.4	>490	55.4
18	0.14	>98.4	>700	60.0
19	0.17	>98.4	>570	>98.4
20	0.098	>98.4	>1000	79.0
21	0.83	20.04	24	>20
22	>28	28.83	<1.0	>28
23	0.16	77.48	484.2	67.93
24	0.0064	>98.0	>15000	57.0
25	0.13	>98.36	>774.0	>98.4
26	0.26	33.45	129.1	>33
28	0.66	>98.4	>141.9	>98.4
63	7.9	61.0	8	>61
64	43.34	>98.4	>2.3	>98.36

^aValues are the mean determined from at least two experiments. Effective concentration for 50% inhibition. ^bConcentration for 50% cytotoxicity. ^cSelective index SI = CC₅₀/EC₅₀.

The antiviral activity of most compounds is similar to the activity of compound **12**. A modification at position 4 or 7 of the benzoxazole ring, keeping the methyl substitution on the pyrimidine ring, does not influence antiviral activity (**17**, **18**, **19**, and **20**). More variations in antiviral activity are observed when the Me is replaced by another substituent. Replacing this by an NH₂ moiety slightly decreases activity (**26**) with concomitant increase of the cytotoxicity. And combining this substitution (NH₂) with a modification on the benzoxazole ring further reduces activity (**21** and **22**). Substituting the methyl for a CH₂OMe or NHCOCH₃ also results in a reduced antiviral activity (**28**, **64**). Introduction of a cyclopropyl (**23**) or isopropyl (**25**) moiety were well tolerated indicating that steric effects may not be an issue. Sulfone derivative (**63**) did also reduce the activity. One modification that results in a very considerable increase of activity is the replacement of the methyl with an ethyl moiety (**24**). This replacement increases the potency by a factor of 17, reaching an EC₅₀ in the low nanomolar range. Compared to the cocrystallized compound **12**, compound **24** is decorated with an ethyl group (same position) that points in the direction of a hydrophobic pocket (F227 in the WT, V106, L234, P236). This hydrophobic pocket seems to be large enough to accept more than a methyl group. The ethyl group may then create more favorable van der Waals interaction than the methyl.

None of the modifications prepared seem to have an influence on the reduced sensitivity of the double mutant (K103N + Y181C). The presence of these mutations reduces the antiviral activity of all compounds at least by a factor of 30.

CONCLUSION

Dramatic enhancements of activity have been reported in many cases for partially fluorinated analogues of biologically active compounds.¹³ This study is another successful example of the potential of this concept by applying it to HIV-1 NNRTI syntheses.

We re-evaluated the antiviral activity of **12** and **13** and tested them against clinically relevant double mutant strains (K103N + Y181C). Our objective was to improve the antiviral activity of the hit **12** using structural biology and medicinal chemistry. The medicinal chemistry effort concentrated on structural modifications on the western wing (benzoxazole) and eastern wing (pyrimidine), keeping the $-\text{CF}_2\text{S}-$ linker intact.

Our efforts in structural biology resulted in a detailed analysis of the binding mode of **12** in the NNRTI pocket of HIV-1, based on two crystal structures obtained by cocrystallization. In comparison with previously published NNRTI-RT crystal structures, the binding of this NNRTI in the pocket involves a H_2O molecule. On the basis of these crystal structures, we synthesized different compounds with the objective of improving the interactions with the enzyme. Our results were successful in the sense that the potency on wild-type HIV-1 (IIIB) could be improved from $\text{EC}_{50} = 110$ nM for **12** to $\text{EC}_{50} = 6.4$ nM for compound **24**. However, none of the compounds showed significant activity on a relevant double mutant NNRTI resistant strain.

Further efforts are necessary to optimize these molecules toward activity on NNRTI-resistant HIV; cocrystallization studies of **24** will be performed in due course in order to propose a model for its better ability to bind to the wild type. Additional derivatives are being investigated with other modifications on the benzoxazole and pyrimidine rings based on our structural biology and current antiviral data. Molecular docking studies combined with our current and new structural biology data will also be planned in order to provide better rationale and support for our hypotheses. The results when available will be presented in a future publication.

EXPERIMENTAL SECTION

Chemistry. Solvents were of the highest purity and anhydrous and were purchased from Acros Organics and Sigma Aldrich. Reagents were used without further purification. ^1H , ^{19}F , and ^{13}C NMR spectra were recorded with a Bruker Avance 300 or a DRX300 spectrometer (in acetone- d_6 , CDCl_3 , or $\text{DMSO}-d_6$) at 300, 282, and 75 MHz, respectively. Chemical shifts are given in parts per million (ppm) relative to the residual peak of solvent ($\delta_{\text{H}} = 7.26$ for CHCl_3 , $\delta_{\text{H}} = 2.50$ for DMSO , $\delta_{\text{C}} = 77.0$ for CDCl_3 and $\delta_{\text{C}} = 39.52$ for $\text{DMSO}-d_6$) or CFCl_3 (^{19}F). The following abbreviations are used to describe peak patterns: s (singlet), d (doublet), dd (double doublet), t (triplet), m (multiplet), q (quadruplet), and br (broad). Coupling constants are given in hertz. Mass spectra were recorded using a Finnigan MAT 95 (electrospray ionization, chemical ionization mode, or electron impact mode). The purities of target compounds were $\geq 95\%$, measured by LC/MS, which was performed on a Waters Acquity UPLC system connected to a Waters Quattro-micro mass spectrometer. Separations were carried out on Waters Acquity BEH (bridged ethylsiloxane/silica hybrid) C18 column ($1.7\ \mu\text{m}$, $2.1\ \text{mm} \times 100\ \text{mm}$) with a flow rate of $0.343\ \text{mL/min}$ at $40\ ^\circ\text{C}$. Two mobile phases (mobile phase A of 95% 7 mM ammonium acetate/ 5% acetonitrile; mobile phase B of 100% acetonitrile) were employed to run a gradient condition from 84.2% A and 15.8% B (hold for $0.49\ \text{min}$) to 10.5% A and 89.5% B in $2.18\ \text{min}$, hold for $1.94\ \text{min}$, and back to the initial conditions in $0.73\ \text{min}$, hold for $0.73\ \text{min}$. An injection volume of $2\ \mu\text{L}$ was used. Cone voltage was $20\ \text{V}$ for positive and negative ionization mode. Mass spectra were acquired by scanning from 100 to 1000 in $0.2\ \text{s}$ using an interscan

delay of $0.1\ \text{s}$. Samples were supplied as $0.5\text{--}1\ \text{mg/mL}$ in methanol and/or acetonitrile with $5\ \mu\text{L}$ injected on a partial loop fill. The purity of the final compounds was determined by HPLC as described above and is 95% or higher unless specified otherwise. Thin-layer chromatography (TLC) was performed on silica gel GF₂₅₄ plates. Macherey-Nagel silica gel 60M ($0.04\text{--}0.063\ \text{mm}$) was used for silica gel chromatography. Solvents for chromatography, workup, and recrystallization are acetone (AC), ethyl acetate (EA), diethyl ether (DE), dichloromethane (DCM), petroleum ether (PE), pentane (PT), hexane (HX), cyclohexane (CY), methanol (ME), absolute ethanol (ET), and chloroform (CL). Melting points (uncorrected) were determined in capillary tubes on a Büchi apparatus.

Typical Procedure for the Preparation of Amino Phenols (38 and 39). **2-Methyl-6-aminophenol (38).** To a solution of $307.5\ \text{mg}$ ($2.01\ \text{mmol}$) of 6-methyl-2-nitrophenol **42** in $40\ \text{mL}$ of methanol and $10\ \text{mL}$ of acetic acid is added $799.6\ \text{mg}$ ($12\ \text{mmol}$) of zinc. This mixture is stirred for $10\ \text{min}$ at room temperature and then filtered. The filtrate is diluted with $60\ \text{mL}$ of water, and the mixture is extracted by $5 \times 80\ \text{mL}$ of diethyl ether. The combined organic layers are then washed with $3 \times 100\ \text{mL}$ of a saturated NaHCO_3 solution, dried over Na_2SO_4 , filtered, and concentrated under reduced pressure. The crude product is purified on a silica gel column (CY/EA = $60:40$). $157.3\ \text{mg}$ (64%) of pure **38** is obtained as a brown viscous oil. ^1H NMR (CDCl_3) δ 6.68 (m, 3H), 3.96 (br, 3H), 2.23 (s, 3H).

6-Chloro-2-aminophenol (39). Yield is 81% from $1.02\ \text{g}$ ($5.76\ \text{mmol}$) of 6-chloro-2- and $2.29\ \text{g}$ ($35\ \text{mmol}$) of zinc (not activated) to afford $666.3\ \text{mg}$ after purification on a silica gel column (PT/EA = $70:30$), brown solid, mp $70\ ^\circ\text{C}$. ^1H NMR (CDCl_3) δ 6.6–6.7 (m, 3H), 5.58 (s, 1H), 3.86 (s, 2H).

2-Amino-3-chlorophenol (40). A suspension of $7.98\ \text{g}$ ($33.1\ \text{mmol}$) of *N*-(2-chloro-6-methoxyphenyl)-2,2-dimethylpropionamide **47** in $190\ \text{mL}$ of HBr is heated to $120\ ^\circ\text{C}$ overnight. After cooling to room temperature, the mixture is diluted with $300\ \text{mL}$ of water. Then $3000\ \text{mL}$ of a 25% aqueous ammonia solution is added to the solution ($\text{pH} > 9$). This mixture is extracted with $4 \times 250\ \text{mL}$ of ethyl acetate. The combined organic layers are dried over Na_2SO_4 , filtered, and concentrated under reduced pressure. The crude product is purified by precipitation from pentane. An amount of $4.37\ \text{g}$ (92%) of pure **39** is obtained as a gray solid, mp $113\ ^\circ\text{C}$. ^1H NMR (CDCl_3) δ 6.82 (m, 1H), 6.64 (m, 1H), 6.55 (m, 1H), 4.60 (br s, 3H).

2-Methyl-6-nitrophenol (42). To a suspension of $2.30\ \text{g}$ of claycop in $14\ \text{mL}$ of carbon tetrachloride and $7\ \text{mL}$ of acetic anhydride is added $1\ \text{mL}$ ($9.52\ \text{mmol}$) of 2-methylphenol. This mixture is stirred $5\ \text{min}$ at room temperature and then filtered. The filtrate is diluted with $50\ \text{mL}$ of dichloromethane, and the mixture is washed with $3 \times 100\ \text{mL}$ of water. The organic layers are dried over Na_2SO_4 , filtered, and concentrated under reduced pressure. The crude product is purified on a silica gel column (CY/EA = $95:5$). An amount of $701.2\ \text{mg}$ (48%) of pure **42** is obtained as a yellowish viscous oil. ^1H NMR (CDCl_3) δ 7.94 (dd, $J = 8.4$ and $0.9\ \text{Hz}$, 1H), 7.43 (dd, $J = 7.2$ and $0.9\ \text{Hz}$, 1H), 6.87 (m, 1H), 2.33 (s, 3H).

***N*-(2-Chloro-6-methoxyphenyl)-2,2-dimethylpropionamide (47).** To a solution of $1.016\ \text{g}$ ($4.91\ \text{mmol}$) of **46** in $10\ \text{mL}$ of dry tetrahydrofuran is slowly added at $-10\ ^\circ\text{C}$, under nitrogen, $4.7\ \text{mL}$ ($11.75\ \text{mmol}$) of a $2.5\ \text{M}$ solution of *n*-BuLi in hexane. This mixture is allowed to warm to room temperature and stirred for $1\ \text{h}$ and $30\ \text{min}$. This solution is then added dropwise under nitrogen to a cooled ($-10\ ^\circ\text{C}$) solution of $1.79\ \text{g}$ ($7.49\ \text{mmol}$) of hexachloroethane in $3.5\ \text{mL}$ of dry tetrahydrofuran. This mixture is stirred $2\ \text{h}$ at $-10\ ^\circ\text{C}$ and then overnight at room temperature. An amount of $50\ \text{mL}$ of water is then added, and that mixture was extracted with $3 \times 50\ \text{mL}$ of dichloromethane. The combined organic layers are dried over Na_2SO_4 , filtered, and concentrated under reduced pressure. The crude product is purified on a silica gel column (HX/EA = $90:10$ to HX/EA = $80:20$). An amount of $770.4\ \text{mg}$ (65%) of pure **47** is obtained as a pale yellowish viscous oil. ^1H NMR (CDCl_3) δ 7.06 (m, 1H), 7.05 (br s, 1H), 6.93 (m, 1H), 6.73 (m, 1H), 3.72 (s, 1H), 1.27 (s, 9H).

Typical Procedure for the Preparation of 2-Bromo-2,2-difluoro-*N*-(2-hydroxy-3-aryl)acetamides (34–37). **2-Bromo-**

2,2-difluoro-*N*-(2-hydroxy-3-methylphenyl)acetamide (34). To a solution of 117.5 mg (0.96 mmol) of **38** in 6 mL of ethyl acetate are added 0.13 mL (0.99 mmol) of ethyl bromodifluoroacetate and 0.15 mL (1.07 mmol) of triethylamine. The reaction mixture is heated at reflux for 5 h. After the mixture is cooled to room temperature, 10 mL of ethyl acetate is added and the solution is washed with 20 mL of dilute HCl (one part concentrated HCl to nine parts of water). The aqueous layer is extracted with 4 × 20 mL of ethyl acetate. The combined organic layers are dried over Na₂SO₄ and concentrated under reduced pressure. The crude product is purified on a silica gel column (CY/EA = 80:20). An amount of 203.1 mg (76%) of pure **34** is obtained as a brown oil. ¹H NMR (CDCl₃) δ 8.45 (br s, 1H), 7.70 (d, *J* = 7.5 Hz, 1H), 7.02 (d, *J* = 7.5 Hz, 1H), 6.89 (m, 1H), 5.90 (br s, 1H), 2.30 (s, 3H). ¹⁹F NMR (CDCl₃) δ -60.6 (s). ¹³C NMR (CDCl₃) δ 157.9 (t, *J* = 54.8 Hz), 144.6 (s), 128.4 (s), 125.3 (s), 123.6 (s), 121.1 (s), 119.3 (s), 111.3 (t, *J* = 314.4 Hz), 15.9 (s). HRMS (CI) calculated for [M + H]⁺ C₉H₉BrF₂NO₂ 279.9785, found 279.9785.

2-Bromo-2,2-difluoro-*N*-(2-hydroxy-3-chlorophenyl)-acetamide (35). Yield is 64%, starting from 139.6 mg (0.97 mmol) of 6-chloro-2-aminophenol **39** and 0.14 mL (1.07 mmol) of ethyl bromodifluoroacetate to afford 187.4 mg of pure **35** after purification on a silica gel column (PE/EA = 90:10), red crystals, mp 54 °C (DCM/HX). ¹H NMR (CDCl₃) δ 8.39 (s, 1H), 8.17 (m, 1H), 7.20 (m, 1H), 6.95 (m, 1H), 5.97 (s, 1H). ¹⁹F NMR (CDCl₃) δ -61.1 (s). ¹³C NMR (CDCl₃) δ 157.3 (t, *J* = 27.8 Hz), 141.2 (s), 125.5 (s), 124.8 (s), 121.6 (s), 119.8 (s), 119.3 (s), 111.2 (t, *J* = 314.7 Hz). HRMS (CI) calculated for [M + H]⁺ C₈H₆BrClF₂NO₂ 299.9239, found 299.9239.

2-Bromo-2,2-difluoro-*N*-(2-hydroxy-6-chlorophenyl)-acetamide (36). Yield is 22% from 4.36 g (30.4 mmol) of 2-amino-2-chlorophenol **40** and 4.4 mL (33.6 mmol) of ethyl bromodifluoroacetate to afford 2.01 g of pure **36** after purification on a silica gel column (HX/EA = 80:20), brown crystals, mp 83 °C (EA/PT). ¹H NMR (CDCl₃) δ 8.40 (br s, 1H), 7.18 (m, 1H), 7.04 (m, 2H), 5.90 (br s, 1H). ¹⁹F NMR (CDCl₃) δ -60.7 (s). ¹³C NMR (CDCl₃) δ 159.2 (t, *J* = 28.2 Hz), 150.9 (s), 129.2 (s), 127.7 (s), 121.8 (s), 120.3 (s), 119.3 (s), 110.6 (t, *J* = 313.5 Hz). HRMS (CI) calculated for [M + H]⁺ C₈H₆BrClF₂NO₂ 299.9239, found 299.9239.

2-Bromo-2,2-difluoro-*N*-(2-hydroxyphenyl)acetamide (37). Yield is 72% from 2.30 g (179 mmol) of **41** and 2.60 mL (199 mmol) of ethyl bromodifluoroacetate to afford a brown powder that is recrystallized (CL/HX) to give 3.89 g of pure **37**, brown crystals, mp 90 °C. ¹H NMR (CDCl₃) δ 7.76 (s, 1H), 7.15 (m, 1H), 6.86 (m, 2H), 6.46 (s, 1H). ¹⁹F NMR (CDCl₃) δ -60.7 (s). ¹³C NMR (CDCl₃) δ 159.2 (t, *J* = 27.8 Hz), 150.6 (s), 134.4 (s), 129.0 (s), 122.9 (s), 120.6 (s), 116.1 (s), 111.1 (t, *J* = 316.1 Hz), 17.7 (s). HRMS (CI) calculated for [M + H]⁺ C₉H₈BrF₂NO₂ 278.9706, found 278.9706.

Typical Procedure for the Preparation of 2-(Bromodifluoromethyl)-Substituted Benzoxazoles. **2-(Bromodifluoromethyl)-7-methylbenzoxazole (29).** A mixture of 210.9 mg (0.75 mmol) of **34** and 0.74 g of polyphosphoric acid is heated at 150 °C for 30 min. Then 9 mL of crushed ice and 2 mL of a 25% aqueous ammoniac solution are added to the flask. After dissolution of the solids, the resulting solution is extracted with 5 × 40 mL of CHCl₃. The combined organic layers are dried over Na₂SO₄, filtered, and concentrated under reduced pressure. The crude product is purified on a silica gel column (CY/EA = 90:10). An amount of 87.7 mg (45%) of pure **29** is obtained as a colorless liquid. ¹H NMR (CDCl₃) δ 7.67 (m, 1H), 7.34 (m, 2H), 2.58 (s, 3H). ¹⁹F NMR (CDCl₃) δ -51.6 (s). ¹³C NMR (CDCl₃) δ 155.4 (t, *J* = 32.1 Hz), 149.9 (s), 139.2 (s), 128.5 (s), 125.8 (s), 122.3 (s), 119.0 (s), 109.0 (t, *J* = 300.3 Hz), 15.0 (s). HRMS (CI) calculated for [M + H]⁺ C₉H₇BrF₂NO 261.9680, found 261.9680.

2-(Bromodifluoromethyl)-7-chlorobenzoxazole (30). Yield is 43%, starting from 1.18 g (3.94 mmol) of **35** and 3.77 g of polyphosphoric acid to afford 479.1 mg of pure **30** after purification on a silica gel column (PT/EA = 95:5), colorless liquid. ¹H NMR (CDCl₃) δ 7.75 (d, *J* = 8.1 Hz, 1H), 7.50 (d, *J* = 7.8 Hz, 1H), 7.40 (m, 1H). ¹⁹F NMR (CDCl₃) δ -52.0 (s). ¹³C NMR (CDCl₃) δ 155.9 (t, *J* = 32.9 Hz), 147.2 (s), 140.7 (s), 128.0 (s), 126.6 (s), 120.2 (s), 117.0

(s), 108.3 (t, *J* = 300.7 Hz). HRMS (CI) calculated for [M + H]⁺ C₈H₄BrClF₂NO 281.9133, found 281.9133.

2-(Bromodifluoromethyl)-4-chlorobenzoxazole (31). Yield is 37% from 386.6 mg (1.29 mmol) of **36** and 1.24 g of polyphosphoric acid to afford 134.2 mg of pure **31** after purification on a silica gel column (HX/EA = 90:10), pale orange solid, mp 35 °C. ¹H NMR (CDCl₃) δ 7.56 (m, 1H), 7.45 (m, 2H). ¹⁹F NMR (CDCl₃) δ -52.4 (s). ¹³C NMR (CDCl₃) δ 156.0 (t, *J* = 33.0 Hz), 151.0 (s), 137.6 (s), 128.2 (s), 126.7 (s), 126.1 (s), 110.2 (s), 108.3 (t, *J* = 300.9 Hz). HRMS (EI) calculated for [M]⁺ C₈H₃BrClF₂NO 280.9055, found 280.9055.

2-(Bromodifluoromethyl)-4-methylbenzoxazole (32). Yield is 80%, starting from 1.84 g (6.57 mmol) of **37** and 6.3 g of polyphosphoric acid to afford 698 mg of pure **32** after purification on a silica gel column (PE/EA = 90:10), colorless liquid. ¹H NMR (CDCl₃) δ 7.43 (m, 2H), 7.27 (m, 1H), 2.67 (s, 3H). ¹⁹F NMR (CDCl₃) δ -51.6 (s). ¹³C NMR (CDCl₃) δ 154.9 (t, *J* = 32.3 Hz), 150.3 (s), 139.0 (s), 132.6 (s), 127.4 (s), 126.2 (s), 108.9 (t, *J* = 300.3 Hz), 108.7 (s), 16.3 (s). HRMS (EI) calculated for [M]⁺ C₉H₆BrF₂NO 260.9601, found 260.9601.

Typical Procedure for the Preparation of Thiopyrimidines (50, 51). **(4-Isopropyl-2-mercaptopyrimidine (50)).** To a mixture of 358.0 mg (2.54 mmol) of (*E*)-1-(dimethylamino)-4-methylpent-1-en-3-one **54** and 218.4 mg (2.84 mmol) of thiourea in 10 mL of absolute ethanol is added 290 mg (5.20 mmol) of sodium methoxide. The reaction mixture is then refluxed in a sealed tube for 24 h. After the mixture is cooled to room temperature, the volatiles are removed under reduced pressure and the crude product is purified on a silica gel column (DCM/ME = 95:5). The yellow solid thus obtained is dissolved in a minimum of dichloromethane and precipitated with pentane. An amount of 149.7 mg (38%) of pure **50** is obtained, yellow solid, mp 86 °C. ¹H NMR (DMSO-*d*₆) δ 13.66 (br s, 1H), 7.98 (d, *J* = 6.0 Hz, 1H), 6.79 (d, *J* = 6.0 Hz, 1H), 2.86 (m, 1H), 1.16 (d, *J* = 6.9 Hz, 6H). ¹³C NMR (DMSO-*d*₆) δ 181.0 (s), 176.1 (s), 158.2 (s), 107.1 (s), 34.8 (s), 20.7 (s). HRMS (CI) calculated for C₇H₁₁N₂S [M + H]⁺ 153.0486 found 153.0484.

4-(Methoxymethyl)-2-mercaptopyrimidine (51). Yield is 38% under reflux for 19 h from 450.5 mg (3.15 mmol) of (*E*)-4-(dimethylamino)-1-methoxybut-3-en-2-one **55** and 267.8 mg (3.48 mmol) of thiourea to afford 128.9 mg of pure **51** after purification on a silica gel column (DCM/ME = 95:5) and precipitation from a MeOH/pentane mixture, yellow solid, mp 152 °C. ¹H NMR (DMSO-*d*₆) δ 13.74 (br s, 1H), 8.05 (d, *J* = 6.0 Hz, 1H), 6.81 (d, *J* = 6.0 Hz, 1H), 4.33 (s, 2H), 3.36 (s, 3H). ¹³C NMR (DMSO-*d*₆) δ 180.5 (s), 175.4 (s), 134.3 (s), 106.0 (s), 58.5 (s), 30.6 (s). HRMS (CI) calculated for C₆H₉N₂OS [M + H]⁺ 157.0436 found 157.0436.

Typical Procedure for the Preparation of 2-[Difluoro-[(substituted-pyrimidinyl)thio]methyl]-Substituted Benzoxazoles. **2-[Difluoro-[(4-methylpyrimidinyl)thio]methyl]-7-methylbenzoxazole (17).** To a suspension of 57 mg (1.43 mmol) of NaH (60% in mineral oil) in 2.5 mL of dry DMF is added under nitrogen 117 mg (0.71 mmol) of 4-methyl-2-mercaptopyrimidine. After 10 min of stirring a solution of 88 mg (0.34 mmol) of 2-(bromodifluoromethyl)-7-chlorobenzoxazole **29** in 2.5 mL of dry DMF is added. The mixture is then heated at 60 °C (oil bath temperature) for 17 h. After the mixture is cooled to room temperature, 15 mL of water is added and the mixture is extracted with 5 × 20 mL of CH₂Cl₂. The combined organic layers are then washed with 3 × 100 mL of water, dried over Na₂SO₄, filtered, and concentrated under reduced pressure. The crude product is purified on a silica gel column (CY/EA = 80:20). An amount of 44.8 mg (43%) of pure **17** is obtained, brown solid, mp 67 °C (CY/PT/DCM). ¹H NMR (CDCl₃) δ 8.23 (d, *J* = 5.1 Hz, 1H), 7.62 (m, 1H), 7.27 (m, 2H), 6.82 (d, *J* = 5.1 Hz, 1H), 2.57 (s, 3H), 2.20 (s, 3H). ¹⁹F NMR (CDCl₃) δ -77.2 (s). ¹³C NMR (CDCl₃) δ 168.2 (s), 166.4 (t, *J* = 5.7 Hz), 157.5 (t, *J* = 31.8 Hz), 157.1 (s), 149.8 (s), 140.0 (s), 127.6 (s), 125.2 (s), 122.0 (s), 120.7 (t, *J* = 271.7 Hz), 118.6 (s), 118.0 (s), 23.7 (s), 15.1 (s). HRMS (CI) calculated for [M + H]⁺ C₁₄H₁₂ClF₂N₃OS 308.0669, found 308.0669. HPLC purity: 97%

2-[Difluoro-[(4-methylpyrimidinyl)thio]methyl]-7-chlorobenzoxazole (18). Yield is 56% at 60 °C for 17 h from 210.0 mg (0.74 mmol) of 2-(bromodifluoromethyl)-7-chlorobenzoxazole **30** and 245 mg (1.53 mmol) of 4-methyl-2-mercaptopyrimidine to afford 136.9 mg of pure **18** after purification on a silica gel column (CY/EA = 80:20), brown solid, mp 66 °C (CY/PT/DCM). ¹H NMR (CDCl₃) δ 8.21 (d, *J* = 5.1 Hz, 1H), 7.69 (m, 1H), 7.45 (m, 1H), 7.35 (m, 1H), 6.82 (d, *J* = 5.1 Hz, 1H), 2.18 (s, 3H). ¹⁹F NMR (CDCl₃) δ -77.8 (s). ¹³C NMR (CDCl₃) δ 168.2 (s), 166.2 (t, *J* = 5.9 Hz), 158.4 (t, *J* = 32.5 Hz), 157.1 (s), 147.1 (s), 141.6 (s), 127.1 (s), 126.0 (s), 120.4 (t, *J* = 272.0 Hz), 119.8 (s), 118.1 (s), 116.6 (s), 23.6 (s). HRMS (CI) calculated for [M + H]⁺ C₁₃H₉ClF₂N₃OS 328.0123, found 328.0123. HPLC purity: 98.2%

2-[Difluoro-[(4-methylpyrimidinyl)thio]methyl]-4-methylbenzoxazole (19). Yield is 80% at 75 °C for 18 h from 197.1 mg (0.75 mmol) of 2-(bromodifluoromethyl)-4-methylbenzoxazole **32** and 251 mg (1.53 mmol) of 4-methyl-2-mercaptopyrimidine to afford 184.6 mg of pure **19** after purification on a silica gel column (PE/EA = 80:20), white solid, mp 80 °C (CY/DCM). ¹H NMR (CDCl₃) δ 8.23 (d, *J* = 5.1 Hz, 1H), 7.42 (m, 1H), 7.33 (m, 1H), 7.19 (m, 1H), 6.82 (d, *J* = 5.1 Hz, 1H), 2.63 (s, 3H), 2.20 (s, 3H). ¹⁹F NMR (CDCl₃) δ -76.8 (s). ¹³C NMR (CDCl₃) δ 168.2 (s), 166.4 (t, *J* = 5.7 Hz), 157.1 (s), 156.9 (t, *J* = 32.1 Hz), 150.3 (s), 139.9 (s), 132.1 (s), 126.5 (s), 125.7 (s), 120.7 (t, *J* = 271.5 Hz), 118.0 (s), 108.5 (s), 23.7 (s), 16.5 (s). HRMS (EI) calculated for C₁₄H₁₂F₂N₃OS 308.0669, found 308.0670. HPLC purity: 97.5%

2-[Difluoro-[(4-methylpyrimidinyl)thio]methyl]-4-chlorobenzoxazole (20). Yield is 47% at 70 °C for 16 h from 2-(bromodifluoromethyl)-4-chlorobenzoxazole **31** and 177 mg (1.08 mmol) of 4-methyl-2-mercaptopyrimidine to afford 82.0 mg of pure **20** after purification on a silica gel column (HX/EA = 80:20), white solid, mp 83 °C (CY/PT/DCM). ¹H NMR (CDCl₃) δ 8.20 (d, *J* = 5.1 Hz, 1H), 7.53 (dd, *J* = 1.8 and 7.5 Hz, 1H), 7.39 (m, 2H), 6.82 (d, *J* = 5.1 Hz, 1H), 2.17 (s, 3H). ¹⁹F NMR (CDCl₃) δ -77.5 (s). ¹³C NMR (CDCl₃) δ 168.2 (s), 166.1 (t, *J* = 6.0 Hz), 158.4 (t, *J* = 32.6 Hz), 157.1 (s), 151.0 (s), 138.5 (s), 127.2 (s), 126.1 (s), 125.6 (s), 120.4 (t, *J* = 271.8 Hz), 118.1 (s), 110.0 (s), 23.7 (s). HRMS (CI) calculated for [M + H]⁺ C₁₃H₉ClF₂N₃OS 328.0123, found 328.0123. HPLC purity: 97.5%

2-[Difluoro-[(4-aminopyrimidinyl)thio]methyl]-4-methylbenzoxazole (21). Yield is 24% at 75 °C for 15 h and 30 min from 178.1 mg (0.68 mmol) of 2-(bromodifluoromethyl)-4-methylbenzoxazole **32** and 180 mg (1.37 mmol) of 4-amino-2-mercaptopyrimidine to afford 50.2 mg of pure **21** after purification on a silica gel column (PE/EA = 60:40), yellow solid, mp 135 °C (CY/DCM). ¹H NMR (CDCl₃) δ 7.84 (d, *J* = 5.7 Hz, 1H), 7.42 (m, 1H), 7.34 (m, 1H), 7.19 (m, 1H), 6.07 (d, *J* = 5.7 Hz, 1H), 2.63 (s, 3H), 2.20 (s, 3H). ¹⁹F NMR (CDCl₃) δ -76.4 (s). HRMS (ESI) calculated for [M + H]⁺ C₁₃H₁₁F₂N₄OS 309.0622, found 309.0622. HPLC purity: 97.4%

2-[Difluoro-[(4-aminopyrimidinyl)thio]methyl]-4-chlorobenzoxazole (22). Yield is 54% at 70 °C for 17 h from 222.0 mg (0.79 mmol) of 2-(bromodifluoromethyl)-4-chlorobenzoxazole **31** and 206.5 mg (1.57 mmol) of 4-amino-2-mercaptopyrimidine to afford 138.6 mg of pure **22** after washing the crude product with pentane, methanol, and diethyl ether, yellow solid, mp (dec) 243 °C (AC). ¹H NMR (acetone-*d*₆) δ 7.80 (d, *J* = 7.5 Hz, 1H), 7.40 (dd, *J* = 1.5 and 8.1 Hz, 1H), 7.31 (m, 1H), 7.20 (dd, *J* = 1.5 and 8.1 Hz, 1H), 6.45 (d, *J* = 7.5 Hz, 1H). ¹⁹F NMR (acetone-*d*₆) δ -66.9 (s). HRMS (CI) calculated for [M + H]⁺ C₁₂H₈ClF₂N₄OS 329.0075, found 329.0074. HPLC purity: 97.8%

2-[Difluoro-[(4-cyclopropylpyrimidinyl)thio]methyl]-benzoxazole (23). Yield is 75% at 70 °C for 15 h from 230.4 mg (0.93 mmol) of 2-(bromodifluoromethyl)benzoxazole and 283.4 mg (1.08 mmol) of 4-cyclopropyl-2-mercaptopyrimidine **48** to afford 224.4 mg of pure **23** after purification on a silica gel column (HX/EA = 80:20), white crystals (CY/PT/DCM), mp 80 °C. ¹H NMR (CDCl₃) δ 8.15 (d, *J* = 5.1 Hz, 1H), 7.81 (m, 1H), 7.62 (m, 1H), 7.43 (m, 2H), 6.84 (d, *J* = 5.1 Hz, 1H), 1.69 (m, 1H), 0.81 (m, 2H), 0.64 (2H, m). ¹⁹F NMR (CDCl₃) δ -77.1 (s). ¹³C NMR (CDCl₃) δ 173.4 (s), 166.4 (t, *J* = 6 Hz), 157.7 (t, *J* = 32 Hz), 156.1 (s), 150.6 (s), 140.4

(s), 126.9 (s), 125.3 (s), 121.4 (s), 120.3 (t, *J* = 271 Hz), 116.7 (s), 111.4 (s), 16.7 (s), 11.7 (s). HRMS (CI) calculated for C₁₅H₁₂F₂N₃OS [M + H]⁺ 320.0669, found 320.0668. HPLC purity: 96.4%

2-[Difluoro-[(4-ethylpyrimidinyl)thio]methyl]benzoxazole (24). Yield is 10% at 70 °C for 15 h from 313 mg (1.27 mmol) of 2-(bromodifluoromethyl)benzoxazole and 350 mg of crude 4-ethyl-2-mercaptopyrimidine **48** to afford 39 mg of pure **24** after purification on a silica gel column (HX/EA = 80:20) and two recrystallizations from CY/PT/DCM, yellowish solid, mp 76 °C. ¹H NMR (CDCl₃) δ 8.25 (d, *J* = 5.4 Hz, 1H), 7.80 (m, 1H), 7.62 (m, 1H), 7.43 (m, 2H), 6.81 (d, *J* = 5.1 Hz, 1H), 2.41 (q, *J* = 7.6 Hz, 2H), 0.94 (t, *J* = 7.6 Hz, 3H). ¹⁹F NMR (CDCl₃) δ -77.5 (s). ¹³C NMR (CDCl₃) δ 173.0 (s), 166.4 (t, *J* = 6 Hz), 157.8 (t, *J* = 32 Hz), 157.2 (s), 150.5 (s), 140.4 (s), 126.8 (s), 125.3 (s), 124.3 (s), 121.4 (s), 120.6 (t, *J* = 271 Hz), 116.9 (s), 111.4 (s), 30.5 (s), 12.0 (s). HRMS (CI) calculated for C₁₄H₁₂F₂N₃OS [M + H]⁺ 308.0669, found 308.0669. HPLC purity: 96.8%

2-[Difluoro-[(4-isopropylpyrimidinyl)thio]methyl]-benzoxazole (25). Yield is 35% at 70 °C for 16 h from 154.0 mg (0.62 mmol) of 2-(bromodifluoromethyl)benzoxazole and 185.7 mg (1.21 mmol) of 4-isopropyl-2-mercaptopyrimidine **50** to afford 69.7 mg of pure **25** after purification on a silica gel column (HX/EA = 80:20), white crystals (CY/PT/DCM), mp 77 °C. ¹H NMR (CDCl₃) δ 8.29 (d, *J* = 5.1 Hz, 1H), 7.80 (m, 1H), 7.62 (m, 1H), 7.43 (m, 2H), 6.81 (d, *J* = 5.1 Hz, 1H), 2.61 (m, 1H), 0.91 (d, *J* = 6.9 Hz, 6H). ¹⁹F NMR (CDCl₃) δ -77.3 (s). ¹³C NMR (CDCl₃) δ 176.8 (s), 166.4 (t, *J* = 6 Hz), 157.8 (t, *J* = 32 Hz), 157.5 (s), 150.6 (s), 140.5 (s), 126.8 (s), 125.3 (s), 121.4 (s), 120.6 (t, *J* = 271 Hz), 115.6 (s), 111.4 (s), 35.6 (s), 21.0 (s). HRMS (CI) calculated for C₁₅H₁₄F₂N₃OS [M + H]⁺ 322.0826, found 322.0826. HPLC purity: 96.7%

2-[Difluoro-[(4-aminopyrimidinyl)thio]methyl]benzoxazole (26). Yield is 80% at 60 °C for 18 h from 157 mg (0.64 mmol) of 2-(bromodifluoromethyl)benzoxazole and 168 mg (1.28 mmol) of 4-methyl-2-mercaptopyrimidine to afford 149 mg of pure **26** after purification on a silica gel column (PE/EA = 60:40), white solid, mp 115 °C (CY/CL). ¹H NMR (CDCl₃) δ 7.86 (m, 2H), 7.64 (d, *J* = 7.5 Hz, 1H), 7.44 (m, 2H), 6.06 (d, *J* = 5.7 Hz, 1H), 4.74 (s, 2H). ¹⁹F NMR (CDCl₃) δ -77.0 (s). ¹³C NMR (DMSO-*d*₆) δ 164.2 (t, *J* = 5.4 Hz), 163.2 (s), 157.0 (t, *J* = 31.8 Hz), 155.0 (s), 150.0 (s), 139.7 (s), 127.5 (s), 125.8 (s), 121.2 (s), 120.8 (t, *J* = 268.3 Hz), 111.9 (s), 103.3 (s). HRMS (EI) calculated for C₁₂H₈F₂N₄OS 295.0465, found 295.0466. HPLC purity: 96.4%

2-[Difluoro-[(4-(methoxymethyl)pyrimidinyl)thio]methyl]-benzoxazole (28). Yield is 50% at 70 °C for 18 h from 84.0 mg (0.34 mmol) of 2-(bromodifluoromethyl)benzoxazole and 101.8 mg (1.21 mmol) of 4-(methoxymethyl)-2-mercaptopyrimidine **51** to afford 55.0 mg of pure **28** after purification on a silica gel column (HX/EA = 80:20), yellowish thick oil. ¹H NMR (CDCl₃) δ 8.36 (d, *J* = 5.1 Hz, 1H), 7.80 (m, 1H), 7.62 (m, 1H), 7.43 (m, 2H), 7.11 (d, *J* = 5.1 Hz, 1H), 4.11 (s, 2H), 3.27 (s, 3H). ¹⁹F NMR (CDCl₃) δ -77.2 (s). ¹³C NMR (CDCl₃) δ 168.8 (s), 166.1 (t, *J* = 6 Hz), 158.0 (s), 157.7 (t, *J* = 32 Hz), 150.5 (s), 140.4 (s), 126.9 (s), 125.3 (s), 121.4 (s), 120.6 (t, *J* = 272 Hz), 115.0 (s), 111.4 (s), 73.4 (s), 58.9 (s). HRMS (CI) calculated for C₁₄H₁₂F₂N₃O₂S [M + H]⁺ 324.0618, found 324.0618. HPLC purity: 97.1%

2-[Difluoro-(4-methylpyrimidin-2-ylsulfonyl)methyl]-benzoxazole (63). An amount of 234 mg (0.8 mmol) of **12** was dissolved in dichloromethane (1 mL), and the resulting pale yellow solution, cooled to 0 °C, is treated dropwise by a dichloromethane solution (8 mL) of 1.1 g (64 mmol) of *m*CPBA (70%). The resulting yellowish-orange solution is then warmed to room temperature and stirred for 15 h. The solution is then filtered and the solid washed with dichloromethane (4 × 2 mL). The combined solutions were evaporated to dryness. The crude product is then purified on a silica gel column (PE/EA = 30:70). An amount of 0.12 g (46%) of pure **63** is obtained, red crystals, mp 110–111 °C. ¹H NMR (CDCl₃) δ 8.70 (d, *J* = 5.1 Hz, 1H), 7.80 (d, *J* = 7.5 Hz, 1H), 7.60 (d, *J* = 8.1 Hz, 1H), 7.50 (m, 3H), 2.60 (s, 3H). ¹⁹F NMR (CDCl₃) δ -103.7 (s). MS *m/z* (%) 674 (29), 673 (2M + 2Na, 100), 348 (M + Na, 58), 326 (M + 1,

11), 168 (12). HRMS (EI) calculated for $C_{12}H_8F_2N_4OS$ 295.0465, found 295.0466. HPLC purity: 97.3%

2-[Difluoro-[(4-(acetamido)pyrimidinyl)thio]methyl]benzoxazole (64). To a solution of 52.8 mg (0.18 mmol) of 2-[difluoro-[(4-aminopyrimidinyl)thio]methyl]benzoxazole **26** in 0.45 mL of pyridine containing 0.43 mL of acetic anhydride is added a catalytic amount of DMAP. The reaction mixture is heated to 55 °C for 7 h. After cooling to room temperature, the mixture is concentrated and the crude is purified on a silica gel column (HX/EA = 60:40). The solid thus obtained is washed with pentane and diethyl ether, and after filtration, 21.2 mg (35%) of pure **64** is obtained, brown solid, mp 183 °C. 1H NMR ($CDCl_3$) δ 8.26 (d, J = 5.7 Hz, 1H), 7.83 (m, 1H), 7.77 (br s, 1H), 7.64 (m, 1H), 7.47 (m, 2H), 2.11 (s, 3H). ^{19}F NMR ($CDCl_3$) δ -77.1 (s). ^{13}C NMR ($DMSO-d_6$) δ 170.7 (s), 164.1 (t, J = 5 Hz), 159.0 (s), 158.2 (s), 156.2 (t, J = 32 Hz), 150.0 (s), 139.5 (s), 127.6 (s), 125.8 (s), 124.2 (s), 120.6 (s), 116.9 (t, J = 271 Hz), 116.9 (s), 107.4 (s), 24.1 (s). HRMS calculated for $[M + H]^+$ $C_{14}H_{11}F_2N_4O_2S$ 337.0572, found 337.0572. HPLC purity: 96.2%

Biology. Antiviral assays and toxicity measurements were performed as described previously.³⁶

The human T lymphotropic virus type 1 transformed human T lymphoblastoid cell line MT4 was kindly provided by Naoki Yamamoto (National Institute of Infectious Diseases, AIDS Research Center, Tokyo, Japan), maintained in RPMI 1640 medium supplemented with 10% heat-inactivated fetal calf serum, 2 mM L-glutamine, 0.1% $NaHCO_3$, and antibiotics (0.02% gentamicin, 0.8% G418), and incubated in a humidified incubator with a 5% CO_2 atmosphere at 37 °C. MT4-LTR-EGFP cells were obtained by transfecting MT4 cells with a selectable construct encompassing the sequences coding for the HIV long terminal repeat (LTR) as a promoter for the expression of enhanced green fluorescent protein (EGFP) and subsequent selection of permanently transfected cells.

HIV-1 IIIB was provided by Guido van der Groen (Institute of Tropical Medicine, Antwerp, Belgium).

The double mutant (K103N + Y181C) was generated by site-directed mutagenesis. Site-directed mutant RT-coding sequence was generated from a pGEM vector containing the HIV-1 clone HXB2 protease- and RT-coding sequence by using a QuikChange site-directed mutagenesis kit (Stratagene) and high-performance liquid chromatography purified primers (Genset Oligos). Plasmid was sequenced to confirm that it contained the desired mutations. Mutant virus was created by recombination of the mutant protease-RT sequence with a protease-RT-deleted HIV-1 HXB2 proviral clone.³⁷

The antiviral activity on HIV-1 (IIIB and the double mutant) was determined in a cell-based virus replication assay. Here MT4-LTR-EGFP cells (150 000 cells/mL) are infected (multiplicity of infection (MOI) of 0.01) in the presence or absence of different inhibitor concentrations. After 3 days of incubation, the amount of virus replication is quantified by measuring the EGFP fluorescence and expressed as the 50% effective concentration (EC_{50}). The toxicity of inhibitors is determined in parallel on mock-infected MT4 cells (150 000 cells/mL) stably transformed with a CMV-EGFP reporter gene and cultured in the presence or absence of test compound concentrations. After 3 days of incubation, cell proliferation is quantified by measuring the EGFP fluorescence and expressed as CC_{50} values (cytotoxic concentration of drug that reduced the viable cell number by 50%).

Structural Biology. The RT gene (HIV-1, BH10 isolate 19+0-3587) was isolated by PCR. Through the construct the peptide sequence was provided with a C-terminal histidine affinity tag. Mutants were made by PCR by amplification using PfuUltra (Stratagene) polymerase of the entire expression vector with help of two complementary oligonucleotides containing the mutation and subsequent digestion with DpnI (Stratagene) of the parental vector, prior to transformation to the cell line TOP10 (Invitrogen) for cloning. Expression was done with help of the vector pCART7 and as described previously.³⁸ The inhibitor complexes were formed by addition of the inhibitor in DMSO solution to a 2-fold molar excess to the RT solution (20 mg/mL). Crystals were produced by vapor diffusion in which an amount of 5 μ L of crystallization buffer (1.4 M

$(NH_4)_2SO_4$, 50 mM Hepes, pH 7.2, 5 mM $MgCl_2$, and 300 mM KCl) was combined with 5 μ L of the protein solution and equilibrated against the crystallization buffer. The droplets were seeded with microcrystals. Crystals appeared after 3 days and grew to a size of 0.3 mm \times 0.2 mm \times 0.2 mm within 1 month. Data were collected at beamline I911-2 at MAX-lab to 2.9 and 2.1 Å for the F227C, E478Q and the F227L, E478Q crystals, respectively (Table 1 in Supporting Information). The two crystal structures were solved with molecular replacement using AMORE and rigid body refinement using Refmac with PDB entries as 1IKX template. The final structures including 276 water molecules and one Ca ion were refined with CNS and Refmac to final R_{free} values (Table 1 in Supporting Information). Amino acids B219-231 and B358-361 could not be traced confidently and were excluded in both structures. The electron densities at the active site including compound **12** are very clear and were unambiguously interpreted early in refinement. The structures were deposited with the PDB with identity codes 2ykm (F227C, E478Q*12) and 2ykn (F227L, E478Q*12).

■ ASSOCIATED CONTENT

Supporting Information

Figures showing new leads, NNRTIs, and Merck pyridinone NNRTIs; schematic of electronic density surrounding Tyr181, Tyr188, and compound **12**; Table 1 containing crystallographic information. This material is available free of charge via the Internet at <http://pubs.acs.org>.

Accession Codes

[†]Protein Data Bank entries are the following: 2ykm (F227C, E478Q*12), 2ykn (F227L, E478Q*12), 3MEE (TMC278).

■ AUTHOR INFORMATION

Corresponding Author

*For M.M: phone: +33 4 7243 1989; e-mail, maurice.medebielle@univ-lyon1.fr. For J.G: phone, +33 2 3261 7458; e-mail, jguillem@its.jnj.com. For J.U: phone, +46 7 0143 6965; e-mail, johan.unge@maxlab.lu.se.

Present Address

[#]Rega Institute for Medical Research, Katholieke Universiteit Leuven, Minderbroedersstraat 10, B-3000 Leuven, Belgium.

■ ACKNOWLEDGMENTS

This investigation was supported by Tibotec Pharmaceuticals and in part by the Centre National de la Recherche Scientifique (CNRS) and Université Claude Bernard Lyon 1. We thank L. Dehuyser for making some additional **12** and **13** and C. Perez for the preparation of **63**. We also thank Torsten Unge for initial crystallographic work and enzyme production. We are grateful to the Centre Commun de Spectrométrie de Masse (CCSM) of Université Claude Bernard Lyon 1 (F. Albrieux, C. Duchet, N. Enriques) for the MS analyses. M.M. thanks Dr. Luc Van Hijfte (Johnson and Johnson Research and Development, Beerse, Belgium) for support at the early stage of this work, Kenny Simmen (Johnson & Johnson Research and Development, Mechelen, Belgium), and Pr. William R. Dolbier, Jr and Dr. Conrad Burkholder (University of Florida, Gainesville, FL, U.S.) for their early contributions to this project.

■ ABBREVIATIONS USED

CC_{50} , concentration for 50% cytotoxicity; DAPY, diarylpyrimidines; DFMB, difluoromethylbenzoxazoles; EC_{50} , effective concentration for 50% inhibition; HAART, highly active antiretroviral therapy; HIV, human immunodeficiency virus; NIH, National Institutes of Health; NNRTI, non-nucleoside

reverse transcriptase inhibitor; PDB, Protein Data Bank; RT, reverse transcriptase; SI, selectivity index (ratio CC_{50}/EC_{50}); TDAE, tetrakis(dimethylamino)ethylene

REFERENCES

- (1) Prajapati, D. C.; Ramajayam, R.; Yadav, M. R.; Giridhar, R. The search for potent, small molecule NNRTIs: a review. *Bioorg. Med. Chem.* **2009**, *17*, 5744–5762.
- (2) Guillemont, J.; Pasquier, E.; Palandjian, P.; Vernier, D.; Gaurrand, S.; Lewi, P. J.; Heeres, J.; De Jonge, M. R.; Koymans, L. M. H.; Daeyaert, F. F. D.; Vinkers, M. H.; Arnold, E.; Das, K.; Pauwels, R.; Andries, K.; De Béthune, M.-P.; Bettens, E.; Hertogs, K.; Wigerinck, P.; Timmerman, P.; Janssen, P. A. Synthesis of novel diarylpyrimidine analogues and their antiviral activity against human immunodeficiency virus type 1. *J. Med. Chem.* **2005**, *48*, 2072–2079.
- (3) Tian, X.; Qin, B.; Wu, Z.; Wang, X.; Lu, H.; Morris-Natschke, S. L.; Chen, C. H.; Jiang, S.; Lee, K.-H.; Xie, L. Design, synthesis, and evaluation of diarylpyridines and diarylanilines as potent non-nucleoside HIV-1 reverse transcriptase inhibitors. *J. Med. Chem.* **2010**, *53*, 8287–8297.
- (4) Ardea Biosciences. <http://www.ardeabio.com/development-pipeline/hiv.htm>.
- (5) Alexandre, F.-R.; Amador, A.; Bot, S.; Caillet, C.; Convard, T.; Jakubik, J.; Musiu, C.; Poddesu, B.; Vargiu, L.; Liuzzi, M.; Roland, A.; Seifer, M.; Standing, D.; Storer, R.; Dousson, C. B. Synthesis and biological evaluation of aryl-phospho-indole as novel HIV-1 non-nucleoside reverse transcriptase inhibitors. *J. Med. Chem.* **2011**, *54*, 392–395.
- (6) Tucker, T. J.; Sisko, J. T.; Tynebor, R. M.; Williams, T. M.; Felock, P. J.; Flynn, J. A.; Lai, M.-T.; Liang, Y.; McGaughey, G.; Liu, M.; Miller, M.; Moyer, G.; Munshi, V.; Perlow-Poehnelt, R.; Prasad, S.; Reid, J. C.; Sanchez, R.; Torrent, M.; Vacca, J. P.; Wan, B.-L.; Yan, Y. Discovery of 3-{5-[(6-amino-1H-pyrazolo[3,4-b]pyridine-3-yl)-methoxy]-2-chlorophenoxy}-5-chlorobenzonitrile (MK-4965): a potent, orally bioavailable HIV-1 non-nucleoside reverse transcriptase inhibitor with improved potency against key mutant viruses. *J. Med. Chem.* **2008**, *51*, 6503–6511.
- (7) Saari, W. S.; Hoffmann, J. M.; Wai, J. S.; Fisher, T. E.; Rooney, C. S.; Smith, A. M.; Thomas, C. M.; Goldman, M. E.; O'Brien, J. A.; Nunberg, J. H.; Quintero, J. C.; Schleif, W. A.; Emini, E. A.; Stern, A. M.; Anderson, P. S. 2-Pyridinone derivatives: a new class of nonnucleoside, HIV-1-specific HIV-1 reverse transcriptase inhibitors. *J. Med. Chem.* **1991**, *36*, 2922–2925.
- (8) Le Van, K.; Cauvin, C.; De Walque, S.; Georges, B.; Boland, S.; Martinelli, V.; Demonté, D.; Durant, F.; Hevesi, L.; Van Lint, C. New pyridinone derivatives as potent HIV-1 non-nucleoside reverse transcriptase inhibitors. *J. Med. Chem.* **2009**, *52*, 3636–3643.
- (9) Medina-Franco, J. L.; Martínez-Mayorga, K.; Juárez-Gordiano, C.; Castillo, R. Pyridin-2(1H)-ones: a promising class of HIV-1 non-nucleoside reverse transcriptase inhibitors. *ChemMedChem.* **2007**, *2*, 1141–1147, and references cited therein.
- (10) Burkholder, C. R.; Dolbier, W. R. Jr.; Médebielle, M. Tetrakis(dimethylamino)ethylene as a useful reductant of some bromodifluoromethyl heterocycles. Application to the synthesis of new gem-difluorinated heteroarylated compounds. *J. Org. Chem.* **1998**, *63*, 5385–5394.
- (11) Burkholder, C. R.; Dolbier, W. R. Jr.; Médebielle, M. The syntheses of nonnucleoside, HIV-1 reverse transcriptase inhibitors containing a CF_2 group. The $S_{RN}1$ reactions of 2-(bromodifluoromethyl)benzoxazole with the anions derived from heterocyclic thiols and phenolic compounds. *J. Fluorine Chem.* **2000**, *102*, 369–376.
- (12) Médebielle, M.; Ait-Mohand, S.; Burkholder, C.; Dolbier, W. R. Jr.; Laumond, G.; Aubertin, A.-M. Syntheses of new difluoromethylene benzoxazole and 1,2,4-oxadiazole derivatives, as potent non-nucleoside HIV-1 reverse transcriptase inhibitors. *J. Fluorine Chem.* **2005**, *126*, 535–542.
- (13) (a) Ojima, I. *Fluorine in Medicinal Chemistry and Chemical Biology*; Blackwell: Oxford, U.K., 2009. (b) Bégué, J.-P.; Bonnet-Delpont, D. *Bioorganic and Medicinal Chemistry of Fluorine*; John Wiley & Sons: Hoboken, NJ, 2008.
- (14) Purser, S.; Moore, P. R.; Swallow, S.; Gouverneur, V. Fluorine in medicinal chemistry. *Chem. Soc. Rev.* **2008**, *37*, 320–330.
- (15) Kirk, K. L. Fluorination in medicinal chemistry: methods, strategies, and recent developments. *Org. Process Res. Dev.* **2008**, *12*, 305–321.
- (16) Hagmann, W. K. The many roles for fluorine in medicinal chemistry. *J. Med. Chem.* **2008**, *51*, 4359–4369.
- (17) Médebielle, M.; Dolbier, W. R. Jr. Nucleophilic difluoromethylation and trifluoromethylation using the tetrakis(dimethylamino)-ethylene (TDAE) reagent. *J. Fluorine Chem.* **2008**, *129*, 930–942.
- (18) Rossi, R. A.; Pierini, A. B.; Peññory, A. B. Nucleophilic substitution by electron transfer. *Chem. Rev.* **2003**, *103*, 71–168.
- (19) Nugent, R. A.; Schlachter, S. T.; Murphy, M. J.; Cleek, G. J.; Poel, T. J.; Wishka, D. G.; Graber, D. R.; Yagi, Y.; Keiser, B. J.; Olmsted, R. A.; Kopta, L. A.; Swaney, S. M.; Poppe, S. M.; Morris, J.; Tarpley, W. G.; Thomas, R. C. Pyrimidine thioethers: a novel class of HIV-1 reverse transcriptase inhibitors with activity against BHAP-resistant HIV. *J. Med. Chem.* **1998**, *41*, 3793–3803.
- (20) Wishka, D. G.; Graber, D. R.; Kopta, L. A.; Olmsted, R. A.; Friis, J. M.; Hosley, J. D.; Adams, W. J.; Seest, E. P.; Castle, T. M.; Dolak, L. A.; Keiser, B. J.; Yagi, Y.; Jeganathan, A.; Schlachter, S. T.; Murphy, M. J.; Cleek, G. J.; Nugent, R. A.; Poppe, S. M.; Swaney, S. M.; Han, F.; Watt, W.; White, W. L.; Poel, T.-J.; Thomas, R. C.; Voorman, R. L.; Stefanski, K. J.; Stehle, R. G.; Tarpley, W. G.; Morris, J. *J. Med. Chem.* **1998**, *41*, 1357–1360.
- (21) Nugent, R. A.; Schlachter, S. T.; Murphy, M. J.; Morris, J.; Thomas, R. C. Preparation of Pyrimidine-thioalkyl and Alkylether Compounds. PCT Int. Appl. WO 95/13267, CAN: 123: 143923, 1994; The Upjohn Company.
- (22) Nugent, R. A.; Wishka, D. G.; Cleek, G. J.; Graber, D. R.; Schlachter, S. T.; Murphy, M. J.; Morris, J.; Thomas, R. C. Preparation of 2-Pyrimidino Alkyl Ethers and Thioethers as Inhibitors of Viral Reverse Transcriptase. CAN: 126: 59967, WO 96/35678, 1996; The Upjohn Company.
- (23) Ding, J.; Das, K.; Moereels, H.; Koymans, L.; Andries, K.; Janssen, P. A. J.; Hughes, S. H.; Arnold, E. Structure of HIV-1 RT/TIBO R 86183 complex reveals similarity in the binding of diverse non-nucleoside inhibitors. *Nat. Struct. Biol.* **1995**, *2*, 407–415.
- (24) Lansdon, E. B.; Brendza, K. M.; Hung, M.; Wang, R.; Mukund, S.; Jin, D.; Birkus, G.; Kutty, N.; Liu, X. Crystal structures of HIV-1 reverse transcriptase with etravirine (TMC125) and rilpivirine (TMC278): implications for drug design. *J. Med. Chem.* **2010**, *53*, 4295–4299.
- (25) Das, K.; Clark, A. D. Jr.; Lewi, P. J.; Heeres, J.; De Jonge, M. R.; Koymans, L. M.; Vinkers, H. M.; Daeyaert, F.; Ludovici, D. W.; Kukla, M. J.; De Corte, B.; Kavash, R. W.; Ho, C. Y.; Ye, H.; Lichtenstein, M. A.; Andries, K.; Pauwels, R.; De Béthune, M.-P.; Boyer, P. L.; Clark, P.; Hughes, S. H.; Janssen, P. A.; Arnold, E. Roles of conformational and positional adaptability in structure based design of TMC125-R165335 (etravirine) and related non-nucleoside reverse transcriptase inhibitors that is highly potent and effective against wild-type and drug-resistant HIV-1 variants. *J. Med. Chem.* **2004**, *47*, 2550–2560.
- (26) Dolbier, W. R. Jr.; Burkholder, C. R.; Médebielle, M. Syntheses of 2-(bromodifluoromethyl)benzoxazole and 5-(bromodifluoromethyl)-1,2,4-oxadiazoles. *J. Fluorine Chem.* **1999**, *95*, 127–130.
- (27) Gigante, B.; Prazeres, A. O.; Marcelo-Curto, M. J.; Cornélis, A.; Laszlo, P. Mild and selective nitration by Claycop. *J. Org. Chem.* **1995**, *60*, 3445–3447.
- (28) Bruyneel, F.; Enaud, E.; Billottet, L.; Vanhulle, S.; Marchand-Brynaert, J. Regioselective synthesis of 3-hydroxyorthanilic acid and its biotransformation into a novel phenoxazinone dye by use of laccase. *Eur. J. Org. Chem.* **2008**, 72–79.
- (29) Pelcman, B.; Olofsson, K.; Schaal, W.; Kalvins, I.; Katkevics, M.; Ozola, V.; Suna, E. Benzoxazoles Useful in the Treatment of Inflammation. WO2007/42816 A1, 2007; Biopolix AB.

- (30) Fitzjohn, S.; Robinson, M. P.; Turnbull, M. D. Preparation of Heterocyclic Compounds as Pesticides. WO 9406777, CAN: 121: 157663, 1994; Zeneca Ltd.
- (31) Kirilova, M. A.; Tsil'ko, A. E.; Mistina, I. A.; Petrov, A. A. Cyclization of substituted 1,3-alkenynes with thiourea. *Khim. Geterotsikl. Soedin.* **1971**, 7, 843–845, . CAN: 76: 25230.
- (32) Duggan, M. E.; Hartman, G. D.; Hoffman, W. F.; Meissner, R. S.; Perkins, J. J.; Askew, B. C.; Coleman, P. J.; Hutchinson, J. H.; Naylor-Olsen, A. M. Preparation of Heterocyclic β -Alanine Derivatives as Integrin Antagonists. WO 98108840, CAN: 128: 217627, 1998; Merck & Co., Inc.
- (33) Al-Shiekh, M. A.; El-Din, A. M. S.; Hafez, E. A.; Elnagdi, M. H. α -Enones in heterocyclic synthesis. Part I. Classical synthetic and environmentally friendly synthetic approaches to alkyl and acyl azoles and azines. *J. Chem. Res.* **2004**, 3, 174–179.
- (34) (a) Bondavalli, F.; Bruno, O.; Presti, E. L.; Menozzi, G.; Mosti, L. An efficient synthesis of functionalized 2-pyridinones by direct route or via amide/enolate ammonium salt intermediates. *Synthesis* **1999**, 1169–1174. (b) Bargagna, A.; Cafaggi, S.; Schenone, P. 9. Reaction of ketenes with N,N-disubstituted α -aminomethylene ketones. X. Synthesis of N,N-disubstituted 6-alkyl-4-amino-3,3-dichloro-3,4-dihydro-2H-pyran-2-ones and of 6-alkyl-4-amino-3-chloro-2H-pyran-2-ones. *J. Heterocycl. Chem.* **1980**, 17, 507–511.
- (35) Zhong, W.; Norman, M. H.; Kaller, M.; Nguyen, T.; Rzasa, R. M.; Tegley, C.; Wang, H.-L. Preparation of 2-Oxopyridin-3-yl Thia(di)azoles as Cdk2 and Cdk5 Kinase Inhibitors for the Treatment of Cell Proliferation-Related Disorders. WO 2004060890, CAN: 141: 140450, 2004; Amgen Inc.
- (36) Jochmans, D.; Deval, J.; Kesteleyn, B.; Van Marck, H.; Bettens, E.; De Baere, I.; Dehertogh, P.; Ivens, T.; Van Ginderen, M.; Van Schoubroeck, B.; Ehteshami, M.; Wigerinck, P.; Götte, M.; Hertogs, K. Indolopyridones inhibit human immunodeficiency virus reverse transcriptase with a novel mechanism of action. *J. Virol.* **2006**, 80, 12283–12292.
- (37) Hertogs, K.; de Béthune, M.-P.; Miller, V.; Ivens, T.; Schel, P.; Van Cauwenberge, A.; Van den Eynde, C.; van Gerwen, V.; Azijn, H.; van Houtte, M.; Peeters, F.; Staszewski, S.; Conant, M.; Bloor, S.; Kemp, S.; Larder, B.; Pauwels, R. A rapid method for simultaneous detection of phenotypic resistance to inhibitors of protease and reverse transcriptase in recombinant human immunodeficiency virus type 1 isolates from patients treated with antiretroviral drugs. *Antimicrob. Agents Chemother.* **1998**, 42, 269–276.
- (38) Lindberg, J.; Sigurdsson, S.; Lowgren, S.; Andersson, H. O.; Sahlberg, C.; Noreen, R.; Fridborg, K.; Zhang, H.; Unge, T. Structural basis for the inhibitory efficacy of efavirenz (DMP-266), MSC194 and PNU142721 towards the HIV-1 RT K103N mutant. *Eur. J. Biochem.* **2002**, 269, 1670–1677.